International Journal of Enhanced Research in Science, Technology & Engineering
ISSN: 2319-7463, Vol. 5 Issue 2, February-2016

Numerical Study of Laminar Film Condensation inside a Vertical Tube Subjected to Wall Non Uniform Heat Flux

Kaoutar Zine-Dine*[1], Youness EL Hammami[1], Rachid Mir[1], Touria Mediouni[1], Sara Armou[1]

[1]Mechanics, Process of Energy and Environment Laboratory,
Ibn Zohr University, ENSA, B.P. 1136, Agadir, Morocco

*E-mail: zinedinekaouthar@gmail.com

ABSTRACT

The purpose of this study is to analyse the combined heat and mass transfer by forced convection in laminar film condensation from steam–gas mixture in the presence of non condensable gas along a vertical tube. The wall is cooled by forced convection in contact with an external fluid (air). The flow is two–dimensional, stationary and laminar. Transfers in the liquid–vapor phase are described by the equations of conservation of mass, momentum, energy and diffusion. Coupling between the equations of two phases is assured by the continuity of the shear stresses, density thermal and mass flow at the liquid vapor interface. The physical properties vary depending on the temperature and mass fraction. The Problem was solved numerically by the implicit finite difference method. The comparison with the numerical results in literature is based on air mass fraction and bulk temperature is in good agreement. The effects of convective cooling coefficient, ambient temperature of fluid, inlet temperature of vapor gas mixture and inlet Reynolds number are discussed.

Keywords: Condensation, Cooling, Heat and mass transfer, Liquid film, Phase change, Tube.

1. INTRODUCTION

The study of heat and mass transfer during condensation from the vapor–gas mixture in a vertical tube is relevant to many industrial applications such as refrigeration engineering, desalination systems, heat exchangers and chemical processing, also condensation of the steam used for cooling the walls of the nuclear reactors. One of the important works on condensation of the pure vapors on plates is that of Sparrow and Gregg [1] used the equations of the boundary layer for the study of the stagnant saturated vapor condensation on a vertical flat plate considering the terms of inertia and convection enthalpy. They show that for high values of the number of liquid Prandtl, the effects of convection term enthalpy are not negligible. Koh et al. [2] have made changes to the model of Sparrow and Gregg concerning water vapor condensation on a vertical isothermal wall, taking into account the shear stress at the liquid–vapor interface. The results show that for liquids with a high Prandtl number, the effect of interfacial stresses is negligible. Louahlia and panday [3–4] analyzed numerically film condensation between two parallel plates by forced turbulent convection of a pure fluid and their non–azeotropic binary mixture. The calculations show that the heat transfer by condensation of pure fluids is higher than that of the mixture of these fluids in the same conditions. They showed that for a large turbulent flow velocity in the liquid and vapor phase heat transfer increases. The calculated results also show that there is not much difference to the tube either horizontal or vertical orientation in case of turbulent condensate [4]. Condensation process of water vapor from the vapor–gas mixtures with non–condensable gas is more complex than that of pure vapor and is an important phenomenon in passive containment cooling systems; because of its build up at the liquid–mixture interface. Siow et al. [5] analyzed the condensation in air–steam mixture in laminar flow along a vertical channel. They found that increasing concentrations of non–condensable gas at the inlet of the channel, causing a decrease in the thickness of the condensate film, the local Nusselt number and the axial pressure gradient. the same authors Siow et al. [6] presented a two–phase model of condensation of a laminar film of a gas–vapor mixture in a non–condensable inclined channel Their results showed that the reduction in Froude number Fr (increase of the inclination angle) causes a thinner thickness and a faster liquid film flow.

Other models have been developed for the case of turbulent flow of gas–vapor mixture [7–8–9]. An experimental and analytical investigation of the condensation of the vapor in forced convection turbulent in the presence of non–condensable gas is extended by Hasanein et al. [7] in order to determine the effects of this last on the condensation of steam in a vertical tube. They calculated the relationship between the thermal resistance of the condensate film and vapor heat resistance to non–condensable gas in the same temperature of the mixture. They also showed that the thermal resistance of the condensate wire is greater for a condition of turbulent gas mixture and relatively low mass fraction of gas $W_{nc} < 0.2$. Groff et al. [8] presented a numerical study of the film condensation from turbulent flow of the gas–vapor mixture in a vertical tube using finite volume method. They showed that increasing of inlet Reynolds produces a thin film near the entrance due to large interfacial shear effects; and the increase of difference temperature inlet–wall produces a thicker film because of a higher rate of condensation. Cha'o and Yan [9] developed a numerical model for the study of condensation in turbulent film in the presence of a non condensable gas on a horizontal tube. Their numerical results showed that a very low number of concentrations of gas non-condensable reduce the coefficient of heat transfer and the thickness of the film. Also; the local heat flux and the film thickness increases as the temperature of the surface of the tube decreases.

Dharma et al. [10] presented a study for laminar film condensation of the water vapor, in the presence of non–condensable gas a high concentration such as moist air flowing in a vertical pipe by laminar forced convection using the implicit finite difference method. They showed that the Nusselt numbers and Reynolds increase with temperature, the relative humidity and the Reynolds number of the gas mixture at the entrance of the tube, but decreases when the mixture inlet pressure increases. The coefficient heat transfer and the rate of condensation decrease considerably in the presence of non–condensable gas with a high percentage. Lebedev et al. [11] performed an experimental study of combined heat and mass transfer in vapor condensation from humid air. They observed an increase in condensation heat transfer with an increase in the relative humidity and velocity of the air.

A relatively recent study, the falling film technique is used in the case of water vapor condensation in the presence of a high concentration of non–condensable gas in a vertical tube is being developed by El Hammami et al. [12]. They showed that the condensation of small concentration of vapors is improved at lower wall temperature and the gas content causes a resistance to heat and mass transfer. Hassaninejad farahani et al. [13] developed a numerical analysis for laminar film condensation from high air mass fraction steam–air mixtures in vertical tube with constant wall temperature. They used a finite volume method to the transformed parabolic governing equations in a set of non–linear algebraic equations. Their results included radial–direction profiles of axial velocity, temperature, air mass fraction, as well as axial variation of film thickness, Nusselt number, interface and bulk temperatures, interface and bulk air mass fraction, and proportion of latent heat transfer.

In this article, the results of the calculation model were validated with those in the literature to verify the accuracy of the numerical procedure developed. The comparison is made with numerical study of Hassaninejad farahani et al. [13]. The objective of the present work is designed to study the effects of non uniform heat flow (effects of heat transfer coefficient and temperature of external fluid) on the condensation process.

2. MATHEMATICAL MODEL

A. Physical model and Assumption

The physical model of the problem is a vertical tube with radius R, Length L and thickness δ_z very low compared to R (Fig.1). The flow is two–dimensional, laminar and symmetrical about the centre line of the tube; at the entrance of the tube arrive a flow of steam and non–condensable gas mixture at uniform temperature T_{in}, uniform velocity u_{in}, uniform pressure P_{in} and relative humidity H_r. The tube wall is cooled by forced convection in contact with an external fluid (air). The following assumptions were made for the mathematical formulation:

- The flow is stationary, incompressible and laminar.
- Boundary layer approximations are valid for both phases.
- Radiation heat transfer, viscous dissipation, pressure gradient and the Dufour and Soret effects are negligible.
- The axial diffusion is negligible compared to convection.
- The gas–liquid interface is in the thermodynamic equilibrium, movable and without wave.
- The effect of the superficial tension of the liquid is negligible.

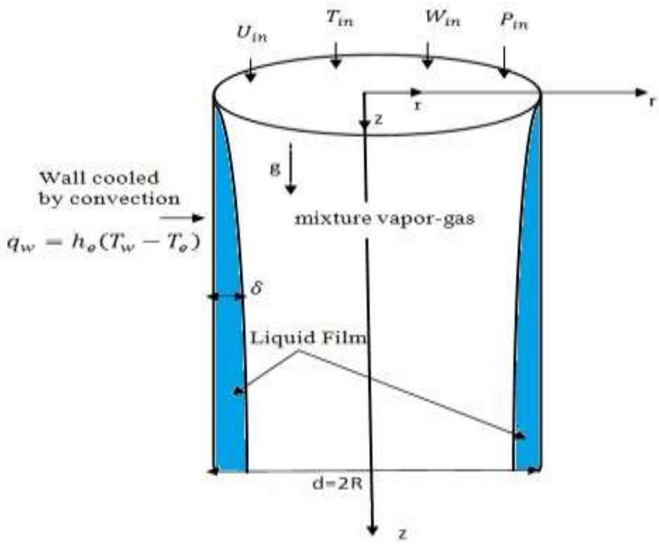

Figure 1: Physical model

The governing equations for the conservation of mass, momentum, energy and diffusion of the physical model with the boundary conditions, in both phase gas and liquid are written for axisymmetric geometry as follows:

1) Liqui Film

Continuity:

$$\frac{\partial}{\partial z}(\rho_l u_l)+\frac{1}{r}\frac{\partial}{\partial r}(r\rho_l v_l)=0 \tag{1}$$

Momentum:

$$\frac{\partial}{\partial z}\left(\rho_l u_l^2\right)+\frac{1}{r}\left(\frac{\partial}{\partial r}(\rho_l r v_l u_l)\right)=-\frac{dP}{dz}+\frac{1}{r}\frac{\partial}{\partial r}\left(r\mu_l\frac{\partial u_l}{\partial r}\right)+\rho_l g \tag{2}$$

Energy:

$$\frac{\partial}{\partial z}\left(\rho_l c_p^l u_l T_l\right)+\frac{1}{r}\frac{\partial}{\partial r}\left(\rho c_p^l r v_l T_l\right)=\frac{1}{r}\frac{\partial}{\partial r}\left(r\lambda_l\frac{\partial T_l}{\partial r}\right) \tag{3}$$

2) Gas Mixture

Continuity:

$$\frac{\partial}{\partial z}(\rho_m u_m)+\frac{1}{r}\frac{\partial}{\partial r}(r\rho_m v_m)=0 \tag{4}$$

Momentum:

$$\frac{\partial}{\partial z}\left(\rho_m u_m^2\right)+\frac{1}{r}\left(\frac{\partial}{\partial r}(\rho_m r v_m u_m)\right)=-\frac{dP}{dz}+\frac{1}{r}\frac{\partial}{\partial r}\left(r\mu_m\frac{\partial u_m}{\partial r}\right)+\rho_m g \tag{5}$$

Energy:

$$\frac{\partial}{\partial z}\left(\rho_m c_p^m u_m T_m\right)+\frac{1}{r}\frac{\partial}{\partial r}\left(\rho_m c_p^m r v_m T_m\right)=\frac{1}{r}\frac{\partial}{\partial r}\left(r\lambda_m\frac{\partial T_m}{\partial r}\right)+\frac{1}{r}\frac{\partial}{\partial r}\left[r\rho_m D\left(c_{p.v}-c_{p.g}\right)\right]\frac{\partial W}{\partial r}T_m \tag{6}$$

Diffusion:

$$\frac{\partial}{\partial z}(\rho_m u_m W)+\frac{1}{r}\frac{\partial}{\partial r}(\rho_m r v_m W)=\frac{1}{r}\frac{\partial}{\partial r}\left(r\rho_m D\frac{\partial W}{\partial r}\right) \tag{7}$$

To complete the mathematical modeling of the problem, it is convenient to add the mass conservation equation in both phase gas and liquid, to transfer equations.

- ✓ The mass conservation equation in the gas is written:

$$\frac{\dot{m}_{in}}{2\pi}=\int_0^{R-\delta_z} r\rho_m u_m dr+\int_0^z \rho_m V_I\left(R-\delta_z\right)dz \tag{8}$$

With

$$V_I = v_i + u_i \frac{d\delta}{dz} = -\frac{D}{1-W_I}\left(\frac{\partial W}{\partial r}\right)_I$$

- ✓ In the liquid material balance is expressed using the following equation:

$$\frac{\Gamma_z}{2\pi} = \int_{R-\delta_z}^{R} r\rho_l u_l dr - \int_0^z \rho_m V_I \left(R-\delta_z\right) dz \tag{9}$$

The thermophysical properties of the liquid film and gas are considered variables depending on the temperature and mass fraction. Complete details for the evaluation of these physical properties of the water, dry air and water vapor are described in Fujii et al. [14].

3) Boundary and Interface Conditions

The equations (1) – (7) are subject to the boundary conditions and interface following:

- Condition at the inlet of the tube $z = 0$

$$u_m = u_{in} \quad T_m = T_{in} \quad W = W_{in} \quad P_m = P_{in} \tag{10}$$

- Condition to the central axis of the tube $r = 0$

  Due to the symmetry

$$\frac{\partial u_m}{\partial r} = 0 \quad \frac{\partial T_m}{\partial r} = 0 \quad \frac{\partial W}{\partial r} = 0 \quad v_m = 0 \tag{11}$$

- Condition in the tube wall $r = R$

$$u_l = v_l = 0 \tag{12}$$

The wall is cooled by convection with an external fluid at temperature T_e:

$$q_w = -\lambda_l \left.\frac{\partial T_l}{\partial r}\right|_w = h_e\left(T_w - T_e\right) \tag{13}$$

- Interfacial conditions $r = R - \delta_z$

Continuities of the velocity and temperature (non-slip condition)

$$u_I\left(z\right) = u_{m,I} = u_{L,I} \qquad T_I\left(z\right) = T_{m,I} = T_{L,I} = T_{sat} \tag{14}$$

Continuities of the shear stress and heat flux

$$\tau_I = \left[\mu_l \frac{\partial u}{\partial r}\right]_{L,I} = \left[\mu_m \frac{\partial u}{\partial r}\right]_{m,I} \tag{15}$$

The heat transfer at the interface can be made by sensitive mode Q_{sI} and latent mode Q_{LI} due to partial condensation of the liquid film. The total heat flow discharged at the surface of the liquid phase to the gas phase is expressed as follows:

$$\left[\lambda_L \frac{\partial T_l}{\partial r}\right]_I = \left[\lambda_m \frac{\partial T_m}{\partial r}\right]_I - \dot{m}_I h_{fg} = Q_{sI} + Q_{LI}$$

(16)

The mass flux exchanged between the two phases is given by Fick's law.

$$\dot{m}_I = \rho_m V_I = -\rho_m D\left(\frac{\partial W}{\partial r}\right)_I \frac{1}{1-W_I} \tag{17}$$

4) Characteristic Variables

The local number Sherwood, along the interface is given by

$$Sh_z = \frac{\dot{m}_I\left(1-W_I\right)\left(2R\right)}{\rho_m D\left(W_b - W_I\right)} \tag{18}$$

With T_b and W_b are respectively the temperature and the mass fraction of the mixture, is given by the following expressions:

$$T_b = \frac{\int_0^{R-\delta} \rho_m c_p^m r u_m T_m dr}{\int_0^{R-\delta} \rho_m c_p^m r u_m dr} \qquad W_b = \frac{\int_0^{R-\delta} \rho_m r u_m W dr}{\int_0^{R-\delta} \rho_m r u_m dr} \tag{19}$$

The total accumulated condensation rate is given by the expression:

$$M_r = \frac{\text{condensate mass flow rate}}{\text{mass flow at the inlet}} = \frac{2\pi \int_0^z (R-\delta_z) \rho_m V_I dz}{\dot{m}_{in}} \tag{20}$$

5) Molar and Mass Fraction at the Interface

In a gas mixture the ideal gas law for each component i is written in the following form:

$$P_i v = \frac{m_i}{M_i} RT \tag{21}$$

In the case of binary mixture of non-condensable gas and steam, the total pressure is:

$$P = P_{nc} + p_v \tag{22}$$

The mass fraction at the interface can be calculated using:

$$W_I = \frac{P_{vs} M_v}{P_{vs} M_v + (P - P_{vs}) M_{nc}} \tag{23}$$

3. NUMERICAL RESOLUTION METHOD

B. Solution Method and Procedure

In view of the impossibility of obtaining an analytic solution for the non-linear coupling differential equations, the conjugated problem defined by the parabolic systems, equation (1) – (7) with the appropriate boundary conditions are solved by a finite difference numerical scheme. The axial convection terms are approximated by the backward difference and the transversal convection and diffusion terms are approximated by the central difference. Each system of the finite-difference equations forms a tridiagonal matrix equation, which can be solved by the TDMA Method [15]. In the centerline (r = 0) of the tube, the diffusional terms are singular. A correct representation can be found from an application of L'Hospital's rule. In this study, the cylindrical coordinate r are transformed into η coordinate system, such that the centre line is at η = 2 the liquid-mixture interface is at η = 1, and the wall is at η = 0. The equations that relate the η coordinate system to the r coordinate system are:

$$\begin{cases} \eta = 2 - \dfrac{r}{R-\delta_z} & \text{for} \quad 0 \le \text{r} \le R-\delta_z \\ \eta = \dfrac{R-r}{\delta_z} & \text{for} \quad \text{R-}\delta_z \le r \le R \end{cases} \tag{24}$$

The resolution of algebraic system resulting from the discretization is effected by an iterative procedure, line by line, with a cross–scan. The solution procedure is outlined as follows:

1. Evaluate the initial values of the dependent variables of thermophysical properties of fluids.
2. Move to next iteration.
3. For any axial location z, guess the values of dP/dz, and δ_z, and solve the equations of momentum to calculate u_l and u_m .
4. Integrate numerically the continuity equation to find v.

$$v_m = -\frac{1}{\rho_m r} \frac{\partial}{\partial z} \int_0^r \rho_m u_m r dr \tag{25}$$

5. Corrected the pressure by using the method of Schneider and Raithby [16], and then correct velocities.
6. Solve the equations of energy and the diffusion.

7. Justify the satisfaction of the conservation of mass in the gas flow and the liquid film. If the following criteria are verified, go to the convergence of the velocity, temperature and the mass fraction of vapor.

$$\frac{\left| \int_0^z 2\pi\left(R-\delta_z\right)V_I\rho_m dz + \int_0^{R-\delta_z} 2\pi r\rho_m u_m dr - \dot{m}_{in} \right|}{\dot{m}_{in}} \prec 10^{-4} \tag{26}$$

$$\frac{\left| \int_0^z 2\pi\left(R-\delta_z\right)V_I\rho_m dz + \int_0^{R-\delta_z} 2\pi r\rho_m u_m dr - \dot{m}_{in} \right|}{\dot{m}_{in}} \prec 10^{-4} \tag{27}$$

If the relative error between two successive iterations to U, T and W satisfy the criteria:

$$\frac{\left|\psi_{i,j}^{n}-\psi_{i,j}^{n-1}\right|_{\max}}{\left|\psi_{i,j}^{n}\right|_{\max}} \prec 10^{-4} \qquad \psi:\{U,T,W\} \tag{28}$$

The solution in each calculation point is complete. If not then repeat steps (2) – (7) until the condition of the equation is (28) justified. If the conditions (26) and (27) are not justified, given dP/dz, δ_z and $\dot{m}_I$, and repeat procedures (2)–(7).

C. Method for Calculating the Liquid Film Thickness

The liquid film thickness is variable along the flow. For each section z, it is calculated by the secant method [17] applied to the equation of total conservation of mass flow condensate. According to the iterative procedure follows:

- Imposing two different arbitrary values of the film thickness δ_1, δ_2.
- For each of them, performs the iterative solution of equations of continuity, momentum, energy and diffusion successively until verification convergence under criterion (28).
- Then calculate the relative error E_n on condensate mass flow rate of.

$$E = 1 - \frac{q_l}{q_c} \tag{29}$$

With q_c is the accumulated mass flow rate by condensation and q_l is the liquid flow:

$$q_c = \int_0^z 2\pi\left(R-\delta_z\right)\rho_m V_I dz \qquad\qquad q_l = \int_{R-\delta}^{R} 2\pi r\rho_l u_l dr$$

- From the third iteration ($n \geq 3$), if the relative error is greater than 10^{-4}, then another value of δ_z is calculated by the secant method as follows:

$$\delta_z^n = \delta_z^{n-1} - E^{n-1}\left(\frac{\delta_z^{n-1}-\delta_z^{n-2}}{E^{n-1}-E^{n-2}}\right) \tag{30}$$

If not, the value obtained δ_z^n is adopted and passed to the next line.

D. Stability of the Calculation Scheme

A preliminary study of choice the computational grid was necessary in the case of a two–phase flow in a vertical tube. To refine the numerical calculation, it is necessary to choose a non–uniform grid using a geometric progression in the axial and radial direction, taking into account the irregular variation of u, W and T at the gas–liquid interface and at the entrance. Therefore, the density of the nodes will be greater at the gas–liquid interface and at the entrance of tube. The radial distribution of nodes of the grids is arranged by locating the first five nodes in the viscous sub–layer of gas at the interface. Table 1. shows the variation of the local Sherwood number sh_z according to the number of chosen points in the axial direction (I) and the direction radial, respectively in the gas (J) and in the liquid (K). It is noted that the differences in the local Sherwood numbers from computations using grids ranging from 51*(81+21) to 201*(121+81) were always less than 3%. In view of these results all further calculations were performed with the 131*(81+31) grid.

Table 1: Comparison of Sherwood number Sh_z for various grids along the tube (Re_{in} =2000, P_{in}=1.atm, T_{in}=60°C and H_r=50%)

	I*(J+K)				
z/L	51*(81+21)	101*(61+31)	131*(81+31)	201*(81+51)	201*(121+81)
0.0470	9.741	9.282	9.290	9.279	9.281
0.3498	5.591	5.583	5.571	5.570	5.580
0.5559	5.160	5.168	5.160	5.162	5.161
0.7531	4.952	4.965	4.950	4.96	4.96
1.00	4.801	4.815	4.808	4.818	4.818

4. VALIDATION OF NUMERICAL CODE

In order to verify the accuracy of the numerical procedure, a computer code were validated by comparing the results obtained on numerical study from the present model and those reported by Hassaninejad farahani et al.[13] in the case of the laminar condensation from a steam–air in a vertical tube at wall temperature T_w=5°C. The first comparison is presented in Fig. 2, which illustrate the evolution of the air mass fraction (a) and dimensionless bulk temperature (b) at various axial. In this comparison inlet pressure P_{in}=1bar, T_{in}=40°C, H_r=100%, L=1m and R=12.5mm. The variation of 1–W in Fig. 2 (a) show that, near the inlet z^*=5, air mass fraction is equal to 1–W_{in} for most of the cross section and the non condensable gas increases rapidly near the interface due to the interface impermeability condition. In Figure 2 (b), the bulk temperature T^*_b decreases along the axial direction, and increases with increasing the Reynolds number Re_{in}. It is observed that the agreement is satisfactory between this study and those of Hassaninejad farahani et al. [13]. The relative gap does not exceed 1.2% in Fig. 2(a) and 6% in Fig. 2(b). This discrepancy is due to the different method used (implicit finite difference method and finite volume method), the type of correlations and thermo physical properties.

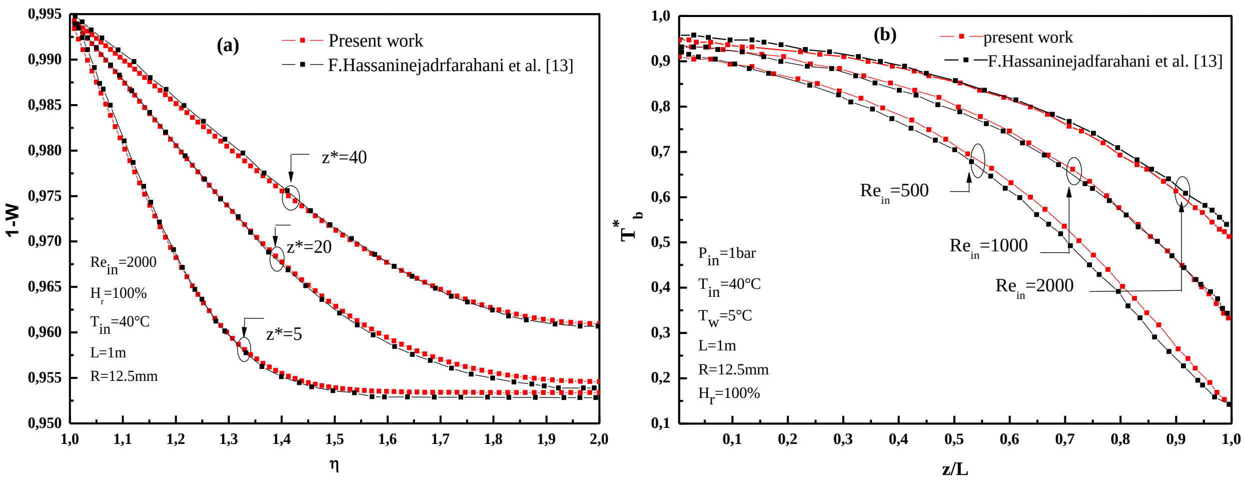

Figure 2: Comparison of air mass fraction (a) and bulk temperature (b) with Hassaninejad farahani [13].

5. RESULTS AND DISCUSSION

In the present work, calculations were made for the case of the condensation steam–air mixture along a vertical tube with length L=2m, diameter d=2cm, relative humidity of vapor mass fraction H_r=50% and inlet pressure P_{in}=1.0atm. Wall is cooled by forced convective in contact with an external fluid (air). The study was performed to examine the effect of convective cooling coefficient h_e and ambient temperature T_e of fluid, effect of inlet temperature of vapor gas mixture T_{in} and effect of inlet Reynolds number Re_{in}. The ranges of each parameter for the analysis are listed in Table

Table 2. The ranges of the physical parameters

Convective coefficient h_e (w/m^2.k)	100 –500
Ambient temperature T_e (°C)	10 – 20
Inlet Temperature T_{in} (°C)	40 – 80
Inlet Reynolds number Re_{in}	500 – 2000

E. Effects of convective coefficient and ambient temperature

Fig. 3 presents the axial variation of interface and bulk vapor mass fraction for three values of convective coefficients h_e and three values of ambient temperatures T_e. Fig. 3(a) shows the effect of the convective cooling coefficient on the axial variation of vapor mass fraction at the interface, this latter decrease with the increase of convective coefficient. This is due to the decreasing of saturation pressure results in a decrease in the interface temperature. Fig. 3(b) presents the axial variation of interface vapor mass fraction. It is noted that the interface vapor mass fraction decrease with decreasing of the ambient temperature T_e of the fluid where the non–condensable gas is more important in view of the condensation of a portion of the water vapor. It is observed that the values of W_I at z/L=0 are dissimilar Fig. 3(b) because of different ambient temperature of external fluid. However, in the Fig. 3(a) the values of W_I is equal to 0.03516 because of same inlet ambient temperature T_e=20°C. The effect of the convective cooling coefficient h_e on the axial variation of bulk vapor mass fraction is shown in the Fig. 3(c). At the beginning the curves are combined and from a value z/L=0.1 the bulk vapor mass fraction decreases with increasing of convective cooling coefficient. However, in Fig. 3(d) the bulk vapor mass decreases with decreasing of ambient temperature. This observation implies that the increase of the temperature difference $\Delta T = T_{in} - T_e$ decreases the bulk vapor mass fraction away from the entrance.

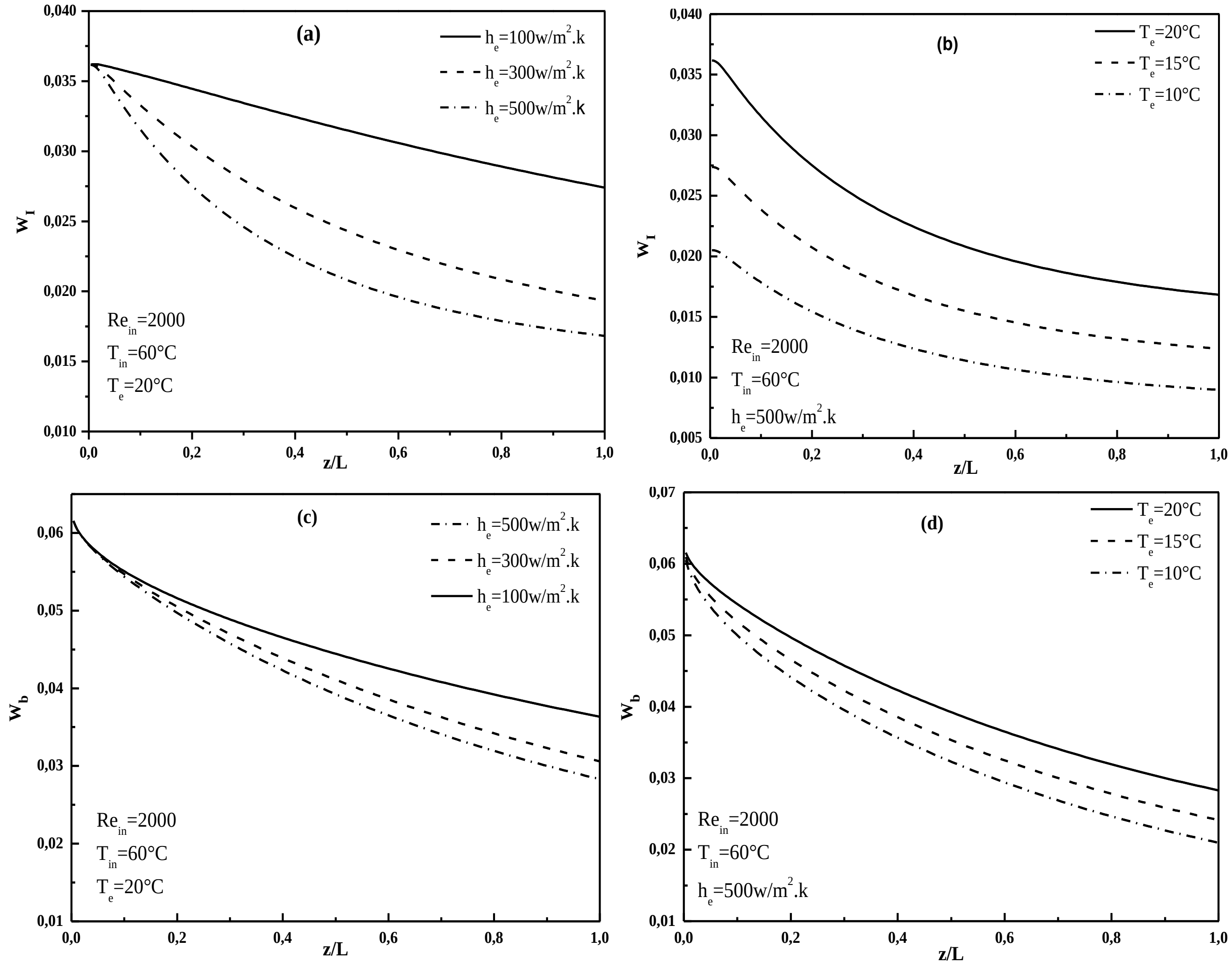

Figure 3: Axial variation of interface and bulk vapor mass fraction along the tube

The influence of the convective coefficient and ambient temperature on the wall, interface and bulk temperature is illustrated in the Fig. 4. Fig. 4(a) shows that the wall and interface temperature are varies in the same manner and decrease along the tube with the increasing of convective coefficient. Indeed, the increase in convective exchange promotes condensation since it causes a more rapid cooling of the wall. The wall and interface temperature decrease with decreasing of the ambient temperature $T_{e;}$ this is implies that the condensation process thus depends strongly on the evolution of the parietal temperature which decreases along the flow and tends asymptotically towards the external ambient fluid temperature Fig. 4(b). On the other hand, the analysis of the influences of heat transfer by convection between the wall and the ambient medium shows that increasing of heat transfer coefficient results in a decrease of the bulk temperature Fig. 4(c). Furthermore, the bulk temperature decreases fairly rapidly along the tub with decreasing of the external ambient fluid temperature Fig. 4 (d).

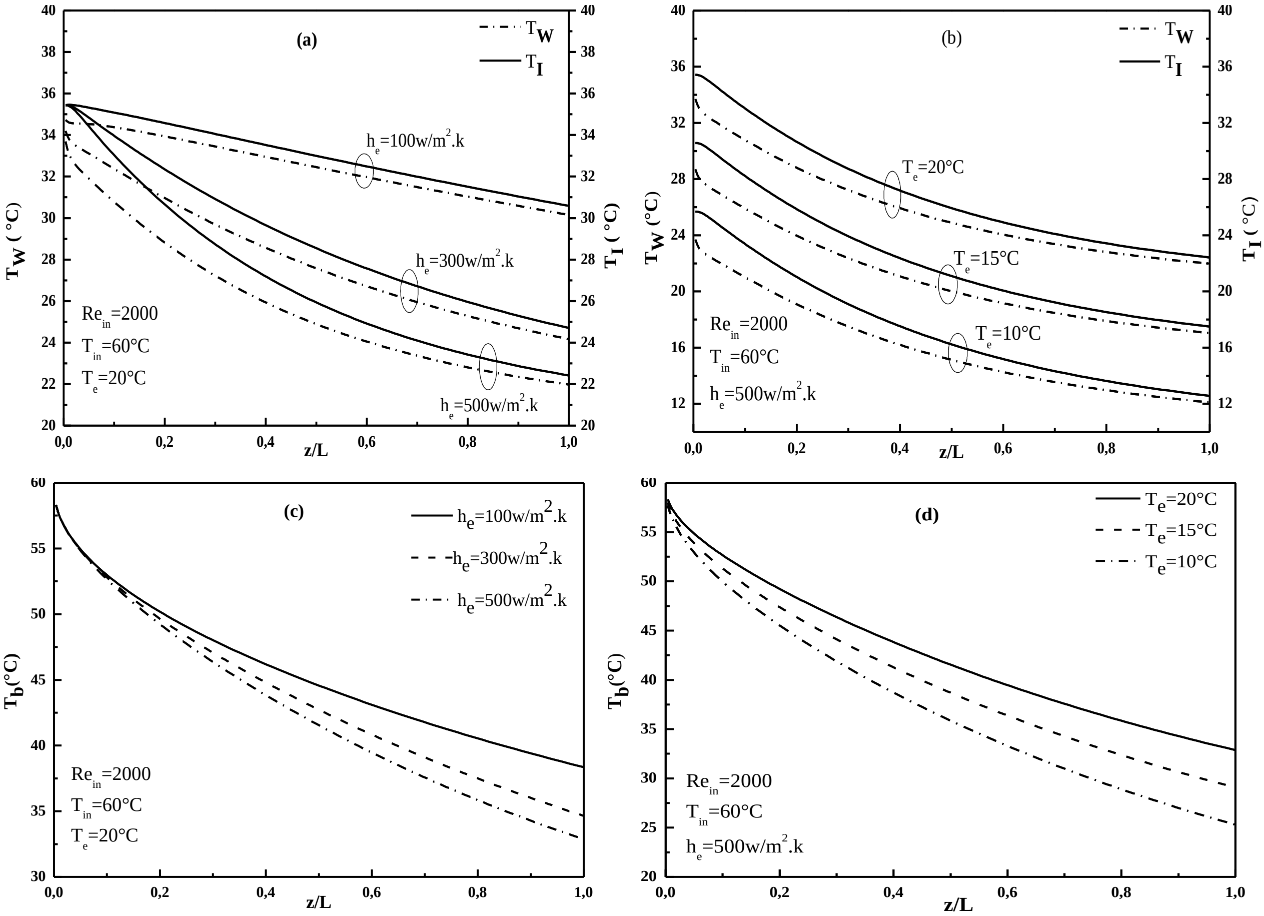

Figure 4: Axial variation of wall, interface and bulk temperature along the tube

F. Effect of Inlet Temperature of Vapor Gas Mixture

Fig.5 (a) shows that the effect of the inlet temperature of vapor gas mixture T_{in} on the axial film thickness for two values of convective coefficient (h_e=100w/m^2.k and h_e=500 w/m^2.k) is insignificant particularly for z/L≤0.2, the liquid film thickness increase with the increasing of inlet temperature of vapor and convective coefficient. Therefore, the condensation requires greater T_{in} and greater h_e in order to condense the maximum vapor. This explains well the significant reduction of the interface vapor mass fraction Fig. 3(a). The evolution of the thickness of the condensed liquid film for three inlet temperature and two ambient temperatures T_e=10°C and T_e=20°C is represented in the Fig. 5(b), it is found that the liquid film thickness increases along the tube, and becomes important for large temperature difference T_{in}–T_e. When the temperature difference increases the heat transfer increases, therefore the density of condensed flow increases. Resulting that the effect of the ambient temperature T_e of the external fluid is more important than the convective coefficient h_e.

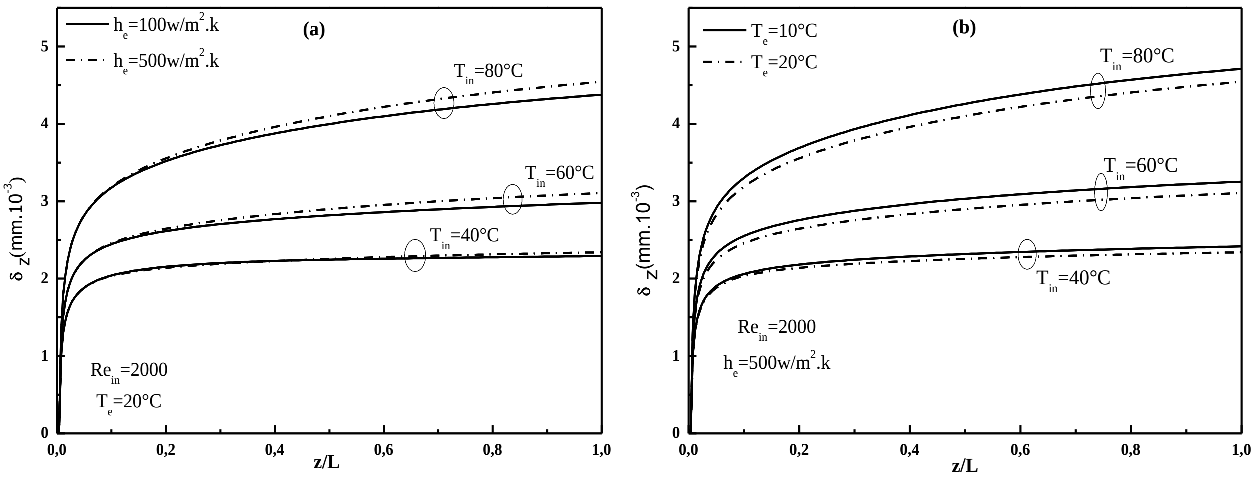

Figure 5: Axial variation of film thickness along the tube for various T_{in}, h_e and T_e

The effect of the inlet temperature of vapor for two values of convective cooling coefficient and two values of ambient temperature on the heat and mass transfer is illustrated in Fig. 6. The mass flow rate normally determines the condensation efficiency. Fig. 6(a) shows the variation of the condensate mass flow along the tube for three values of T_{in}. Near the entrance, $\dot{m}_I$ increases with increasing of T_{in} and increasing of h_e and then decreases faster in the flow at the end of condensation. In the case of T_{in}=40°C the condensate mass flow is very small because the difference between the liquid temperature and inlet temperature of vapor is very small and which does not exceed 5°C, therefore the heat exchanged is very small. Influence of inlet and ambient temperature on the condensate mass flow is illustrated in Fig. 6(b). It is found that the mass flow rate is important for large values of T_{in}–T_e and decreases along the tube toward the case of end of condensation at the exit. This explains why condensation is favored for the large values T_{in}–T_e. This is confirmed by Fig. 5(b) shows increasing the thickness of the condensate δ_z with T_{in}–T_e along the tube.

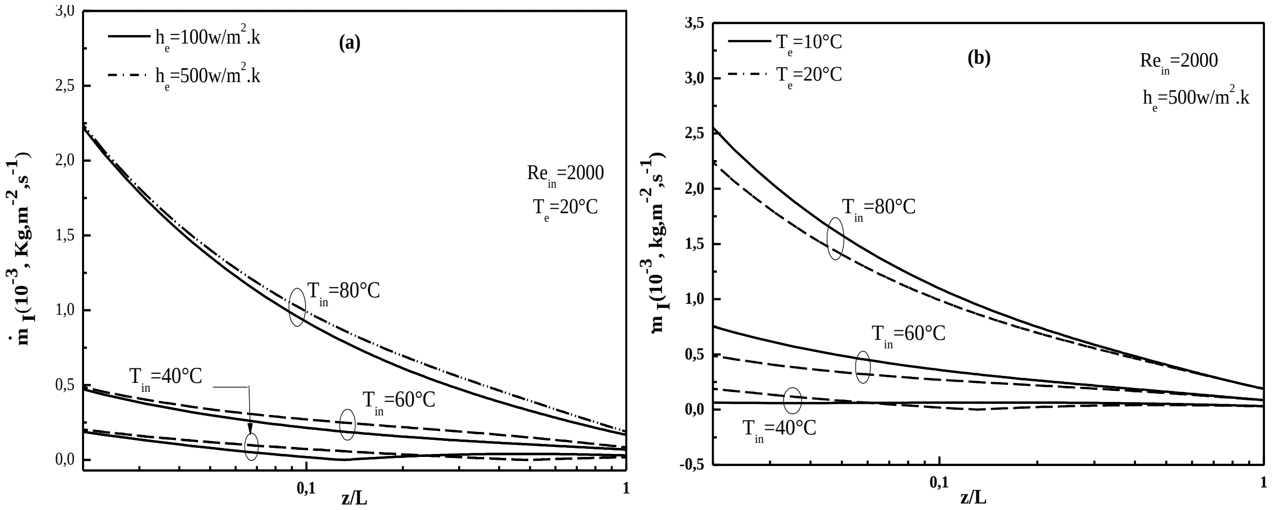

Figure 6: Variation of interfacial mass condensation rat $\dot{m}_I$ along the tube for various h_e, T_e and T_{in}

Fig. 7 illustrates the total condensate rate for water vapor in binary mixture along the tube for different inlet temperature, different convective coefficient and different ambient temperature. It is noted that the condensate rate increases by increasing of the T_{in} and h_e Fig. 7(a). That is to say increasing of vapor mass fraction which explains that water vapor condenses more by reducing the quantity of non–condensable gas. The effect of the external ambient fluid temperature T_e is presented in Fig. 7(b). The condensate rate increases with increasing of T_{in} and decreasing of T_e. This implies that the heat and mass transfer are more effective for small ambient temperature. This finding is very marked on the evolution of the thickness of the condensate (Fig. 5).

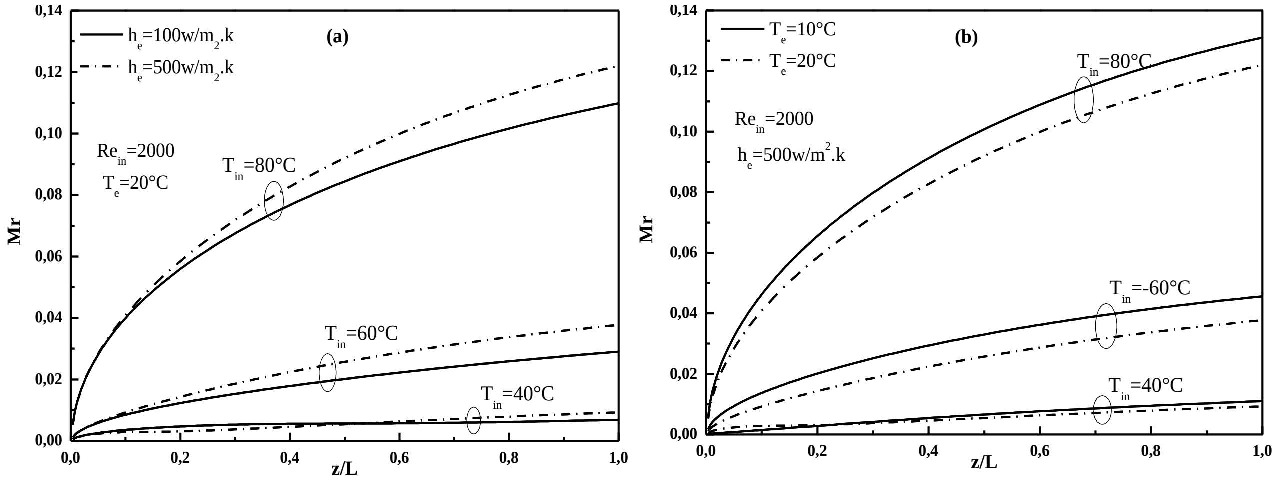

Figure 7: Axial variation of condensate rate M_r along the tube for various T_{in}, h_e and T_e

G. Effect of Inlet Reynolds Number

The effect of inlet Reynolds number Re_{in} on the condensation with wall cooling by convection was investigated for two values (h_e=100w/m^2.k and h_e=500w/m^2.k) and two values (T_e=10°C and T_e=20°C) is plotted in Fig. 8. The curve of film thickness δ_z along the tube increase in a manner very fast with the increase of Reynolds number and it becomes more important for a large value of h_e Fig. 8(a) and small value of T_e Fig. 8(b). This implies that the interfacial shear becomes less significant and the film is thicker for higher inlet Reynolds number. This means that the heat and mass transfer are more effective in forced convection.

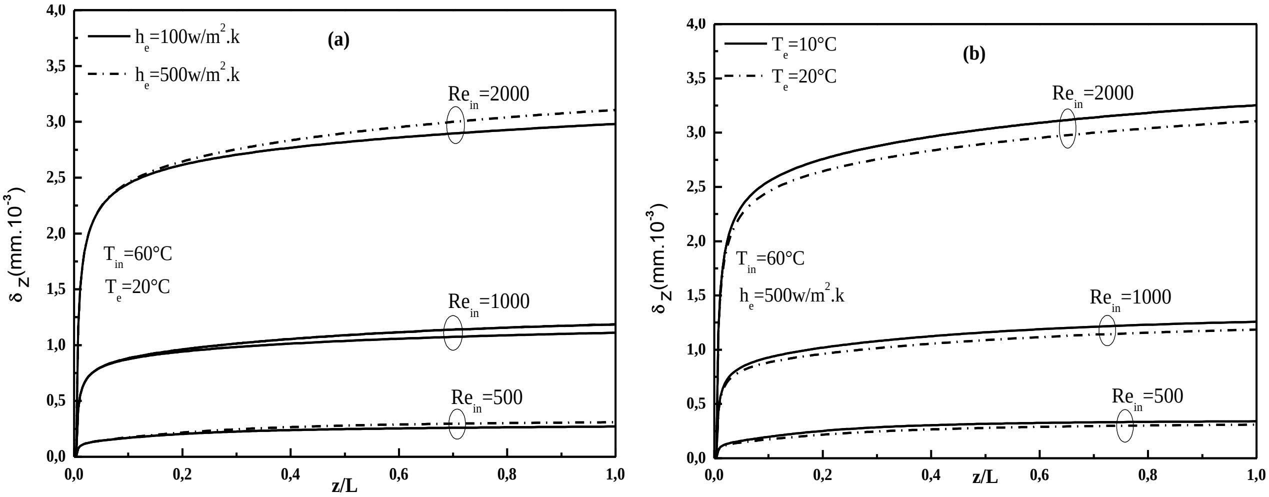

Figure 8: Axial variation of film thickness along the tube for various Re_{in}, h_e and T_e

Fig. 9 shows the variation of condensate mass flow rate for two Reynolds number. At inlet of the tube mass flow rate is very large and increase by increasing of Re_{in} and h_e Fig. 9(a) but it decrease very rapidly towards zero for Re_{in}=500 at end of condensation. This implies that heat and mass transfer are noticeable for higher inlet Reynolds number. Fig. 9(b) illustrates the effect of ambient temperature, for a small value of T_e and near the entrance the mass flow rate of vapor is very large. It is noted that the increase in the Reynolds number influence the condensate mass flow, which is explained by the increasing of the heat exchanged.

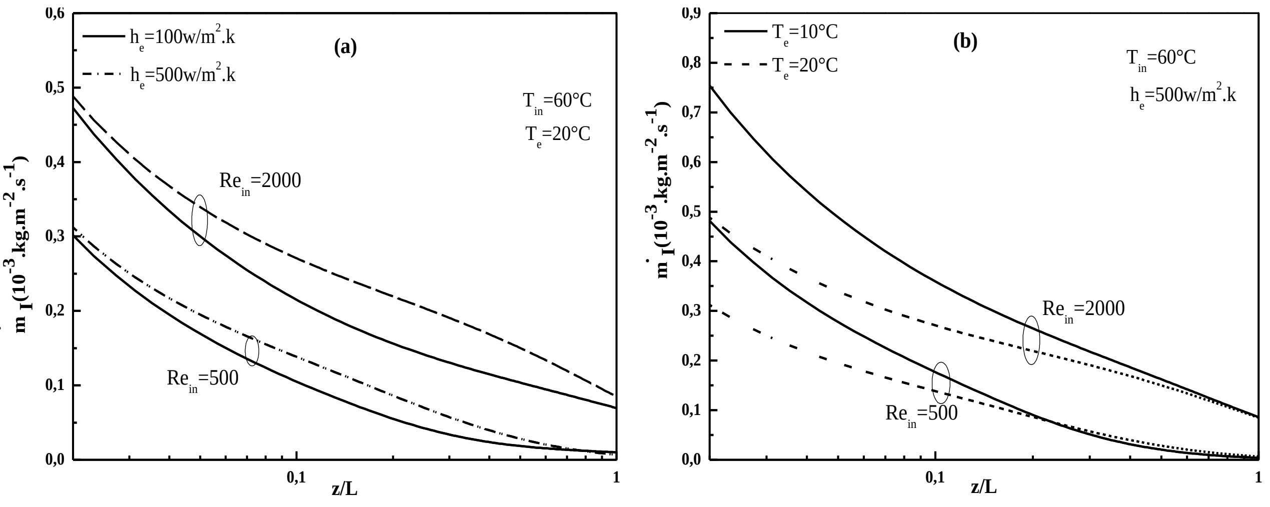

Figure 9: Variation of interfacial mass condensation rat $\dot{m}_I$ along the tube for various h_e, T_e and Re_{in}.

Influence of the Reynolds number, convective coefficient and ambient temperature on the condensate rate M_r along the tube is illustrated in Fig. 10. Fig. 10(a) shows that the condensate rate increases by decreasing of the Reynolds number and it is larger for a large value of convective coefficient h_e and small ambient temperature T_e Fig. 10(b). This means that condensation in the presence of non–condensable gas requires greater convective coefficient in order to condense the maximum vapor and the lower ambient temperature of the external fluid promotes condensation since it causes a more rapid cooling of the wall.

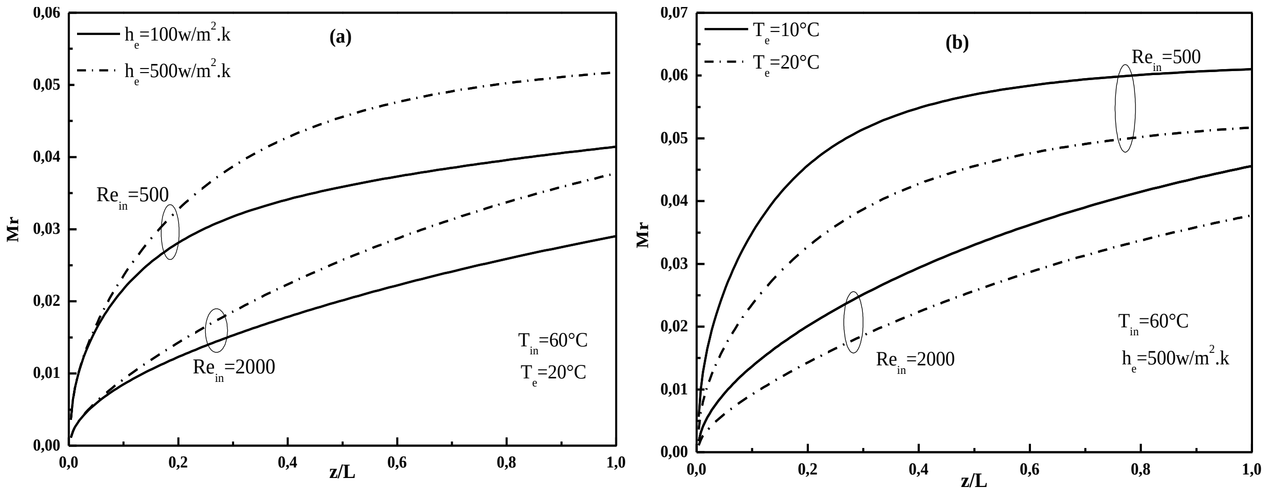

Figure 10: Axial variation of condensate rate M_r along the tube for various h_e, T_e and Re_{in}.

6. CONCLUSIONS

A numerical simulation is presented for laminar film condensation inside a vertical tube with wall is cooled by forced convection in contact with an external fluid (air). Governing equations are discretized by the finite difference method and solved using tridiagonal matrix algorithm. Results were obtained for steam–air mixtures by specifying the following values at the inlet to the tube and the cooling parameters: Pressure, Reynolds number, temperature, relative humidity, convective coefficient and ambient temperature. The study leads to the following conclusions:

1. Condensation is more important for a large convective coefficient h_e=500w/m^2.k and a small ambient temperature T_e=10°C. because its causes a more rapid cooling of wall tube,
2. The cooling of the wall tube favored the process of condensation, and the liquid film thickness, the condensate flow and the mass flow rate are important for a large values of h_e and a large values of difference temperature ΔT.
3. The liquid film thickness and the condensate flow increases strongly at the inlet of the tube, then tend asymptotically toward the limit values corresponding to the condensation end system.
4. The increasing of the inlet Reynolds number influences on the condensate mass flow rate and the film thickness, which is explained by the increase of convective heat exchange between the tube and the medium exterior.

REFERENCES

[1]. E.M., Sparrow J.L., Gregg A Boundary-Layer Treatment of Laminar-Film Condensation, Journal of Heat Transfer, Trans. ASME, Series C, Vol. 81, (1959). pp. 13-18,
[2]. J.C.Y., Koh E.M Sparrow., J.P. Hartnett The Two Phase Boundary Layer in Laminar Film Condensation, International Journal of Heat and Mass Transfer, Vol. 2, (1961). pp. 69-82.
[3]. H.Louahlia, P.K. Panday (1996).Transfert thermique pour la condensation du R123, du R134a et de leurs mélanges en écoulement forcé entre deux plaques planes horizontales: Etude numérique, Rev. Gén. Therm., Vol. 35, pp.615–624.
[4]. P.K. Panday. Two-dimensional turbulent film condensation of vapours flowing inside a vertical tube and between parallel plates: a numerical approach, Int. Journal of Refrigeration 26, (2003). pp.492-503.
[5]. E. C. Siow, S. J. Ormiston, H. M. Soliman A two-phase model for laminar film condensation from steam-air mixtures in vertical parallel-plate channels. Heat and Mass Tran, 40. (2004).
[6]. E. C. Siow, S. J. Ormiston, H. M. Soliman Two-phase modelling of laminar film condensation from vapour-gas mixtures in declining parallel-plate channels. Int J of Thermal Sciences, 46(2007).
[7]. H. A. Hasanein, M. S. Kazimi, M. W. Golay Forced convection in-tube steam condensation in the presence of non-condensable gases, International Journal of Heat and Mass Transfer Vol. 39, No. 13, (1996).pp. 2625-2639.
[8]. M.K., Groff, S.J.Ormiston, H.M. Soliman Numerical solution of film condensation from turbulent flow of vapor–gas mixtures in vertical tubes, International Journal of Heat and Mass Transfer 50, pp. 3899–3912.
[9]. Cha'o-Kuang Chen, Yan-Ting Lin. (2009) Turbulent film condensation in the presence of non-condensable gases over a horizontal tube. International Journal of Thermal Sciences 48 1777–1785.(2007)
[10]. V.Dharma Rao, V.Murali Krishna, K.V.Sharma, P.V.J. Mohana Rao Convective condensation of vapor in the presence of a non-condensable gas of high concentration in laminar flow in a vertical pipe. International Journal of Heat and Mass Transfer 51 6090–6101. (2008).
[11]. P. D Lebedev, A M., Baklastov F. Z. Sergazin Aerodynamics heat and mass transfer in vapour condensation from humid air on a flat plate in a longitudinal flow in asymmetrically cooled slot. Int J Heat Mass Transf, 12. (1969).
[12]. Y. El Hammami, M.Feddaoui, T.Mediouni, & A. Mir Numerical study of condensing a small concentration of vapour inside a vertical tube Heat and Mass Transfer 48: 1675-1685, (2012)

[13]. F.Hassaninejadfarahani, M.K. Guyot,S.J. Ormiston Numerical analysis of mixed convection laminar film condensation from high air mass fraction steam–air mixtures in vertical tubes. International Journal of Heat and Mass Transfer 78 170–180. (2014).
[14]. T.Fujii, Y.Kato, K. Mihara Expressions of transport and thermodynamic properties of air, stream and water, Sei San Ka Gaku Ken Kyu Jo. Report N° 66, Kyu Shu University. Kyu Shu Japan, (1977), pp. 81-95.
[15]. S. V. Patankar Numerical Heat Transfer and Fluid Flow, Hemisphere/Mc Graw-Hill, New York.Chap.6. (1980),
[16]. G. D. Raithby, G. E. Schneider Numerical solutions of problems in incompressible fluid flow: treatment of the velocity-pressure coupling, Numerical Heat Transfer, vol. 2, (1979), pp. 417-440
[17]. J.P. Nougier Méthodes de calcul numérique. Ed. Masson (1991).